



Original Article

Mitochondrial Divergence between Western and Eastern Great Bustards: Implications for Conservation and Species Status

Aimee Elizabeth Kessler, Malia A. Santos, Ramona Flatz, Nyambayar Batbayar, Tsevenmyadag Natsagdorj, Dashnyam Batsuuri,* Fyodor G. Bidashko,* Natsag Galbadrakh,* Oleg Goroshko,* Valery V. Khrokov*, Tuvshin Unenbat,* Ivan I. Vagner,* Muyang Wang,* and Christopher Irwin Smith

From the Eurasian Bustard Alliance, PO Box 2705, Jackson, WY 83001 (Kessler); the Department of Biology, Willamette University, Salem, OR (Santos, Flatz, and Smith); the Wildlife Science and Conservation Center of Mongolia, Ulaanbaatar 14210, Mongolia (Batbayar); the Institute of General and Experimental Biology, Mongolian Academy of Sciences, Ulaanbaatar, Mongolia (Natsagdorj); the Department of Environment & Biodiversity, HSESC, Oyu Tolgoi LLC, Ulaanbaatar, Mongolia (Batsuuri); the Uralsk Anti-Plague Station, Uralsk, Kazakhstan (Bidashko); the Ulaanbaatar Environmental Department, Ulaanbaatar, Mongolia (Galbadrakh); the Daurky State Nature Biosphere Reserve, Chita, Russia (Goroshko); the Institute of Nature Resources, Ecology and Cryology, Russian Academy of Sciences, Chita, Russia (Goroshko); the Association for the Conservation of Biodiversity in Kazakhstan, Astana, Kazakhstan (Khrokov); the Mongolian Ornithological Society, Ulaanbaatar, Mongolia (Unenbat); the Hunters' and Fishers' Society of Southern Kazakhstan Province, Shymkent, Kazakhstan (Vagner); the Key Laboratory of Biogeography and Bioresources in Arid Lands, Xinjiang Institute of Ecology and Geography, Chinese Academy of Sciences, Urumqi, China (Wang). Malia A. Santos is now at the University of Idaho, 875 Perimeter Drive, Moscow, ID 83844.

Address correspondence to A. E. Kessler at the address above, or e-mail: mimi@asiangreatbustard.org.

Received November 20, 2017; First decision May 7, 2018; Accepted June 1, 2018.

Corresponding Editor: Alfred Roca

*These authors contributed identically and are listed in alphabetical order.

Abstract

The great bustard is the heaviest bird capable of flight and an iconic species of the Eurasian steppe. Populations of both currently recognized subspecies are highly fragmented and critically small in Asia. We used DNA sequence data from the mitochondrial cytochrome b gene and the mitochondrial control region to estimate the degree of mitochondrial differentiation and rates of female gene flow between the subspecies. We obtained genetic samples from 51 individuals of *Otis tarda dybowskii* representing multiple populations, including the first samples from Kazakhstan and Mongolia and samples from near the Altai Mountains, the proposed geographic divide between the subspecies, allowing for better characterization of the boundary between the 2 subspecies. We compared these with existing sequence data ($n = 66$) from *Otis tarda tarda*. Our results suggest, though do not conclusively prove, that *O. t. dybowskii* and *O. t. tarda* may be distinct species. The geographic distribution of haplotypes, phylogenetic analysis, analyses of molecular variance,

and coalescent estimation of divergence time and female migration rates indicate that *O. t. tarda* and *O. t. dybowskii* are highly differentiated in the mitochondrial genome, have been isolated for approximately 1.4 million years, and exchange much less than 1 female migrant per generation. Our findings indicate that the 2 forms should at least be recognized and managed as separate evolutionary units. Populations in Xinjiang, China and Khövsgöl and Bulgan, Mongolia exhibited the highest levels of genetic diversity and should be prioritized in conservation planning.

Keywords: coalescent, female gene flow, IMA2, isolation, mitochondrial DNA, Otidae, *Otis tarda*, speciation

Breeding populations of the great bustard (*Otis tarda* Linnaeus, 1758) can be found across temperate Eurasia, from Portugal to Manchuria. This species is the heaviest bird capable of flight, reaching weights of nearly 20 kg on a diet of invertebrates and vegetation (Rocha et al. 2005; Dunning 2008). The great bustard also displays the largest sexual size dimorphism in birds, with males 2.5 times heavier than females (Alonso et al. 2009). Discrete populations of this lekking species gather each spring at traditional sites to perform elaborate breeding displays (Collar 1996). The great bustard is a species of conservation concern, listed as vulnerable worldwide (BirdLife International 2016, A2cd+3cd+4cd, ver 3.1), but with considerable variation in population status across its broad range and between subspecies. An effective conservation plan for any such species with so wide a range needs to be based on sound evidence of the degree of genetic variation that may exist between populations and needs to address management proposals for any evolutionarily significant units that can be identified.

Taxonomic identification of great bustards in Asia has been revised over the past century. Currently, 2 subspecies are recognized which are separated by the Altai Mountain range in eastern Central Asia. The eastern subspecies (*Otis tarda dybowskii*, “Asian great bustard”) was originally proposed as a distinct species by Taczanowski (1874), who described morphometric and plumage differences from the nominate (*Otis tarda tarda*, “Western great bustard”). This form was later relegated to subspecies level. A third subspecies, *Otis tarda korejewi*, inhabiting Central Asia, was described on the basis of plumage differences (Sarudny 1905) but was later incorporated into *O. t. tarda* (Spangenberg 1951; Vaurie 1965).

Otis tarda tarda and *O. t. dybowskii* exhibit differences in both plumage and ecology. Plumage differences involve coloration of the wing coverts, rectrices and mantle, and the distribution of facial plumes used in courtship (Taczanowski 1874; Ivanov et al. 1951; Spangenberg 1951; Vaurie 1965; Etchécopar 1978; Roselaar 1980; Wang and Yan 2002). Ecologically, the Asian great bustard inhabits a more severe climate. For example, the mean annual range in temperature in Spain is similar to the mean daily range of temperature in Mongolia during the breeding season alone (20 °C; Linés Escardó 1970; Lydolph 1977). Asian great bustards accommodate a shorter breeding season than the nominal subspecies, typically experiencing a frost-free period of 90–105 days, compared with 150–165 days in the Volga River region and 200–250 days in Spain; Linés Escardó 1970; Lydolph 1977; Schüepp and Schirmer 1977). As a result, the breeding season of Asian great bustards begins later, chicks must fledge more quickly, and adults must prepare for migration over the more compressed period of time during which higher-quality insect food and forage is available. Asian Great Bustards perform a migratory journey twice the length of that recorded for any population of the nominate subspecies (Kessler et al. 2013). In addition to the dry, open grasslands and cereal agriculture typically described as habitat

for the nominate subspecies, the Asian great bustard also breeds in small openings in taiga forest and moist depressions with higher vegetation growth (Spangenberg 1951; Goroshko 2008; Kessler 2015). Although observations of the nominate subspecies of great bustard near trees are incidental, it is not uncommon for Asian great bustards to nest at the forest edge (Raab et al. 2014; Kessler 2015).

The conservation status of the 2 subspecies is drastically different, although populations of both are at critically low levels in Asia. The breeding range of *O. t. dybowskii* is restricted to eastern Siberian Russia, Mongolia, and Inner Mongolia, China, where approximately 1500 individuals remain. In comparison, 42000–55000 individuals of *O. t. tarda* are estimated to remain in a range stretching from Portugal to Xinjiang, western China (Alonso and Palacín 2010; BirdLife International 2016). The bulk of this population is found in Europe, with only approximately 500 individuals of *O. t. tarda* remaining across an east-west distribution of 2500 km in Central Asia (breeding in south-central Siberian Russia, Kazakhstan, and Xinjiang), where populations are often small and isolated by hundreds of kilometers (Alonso and Palacín 2010; Kessler and Smith 2014).

To date, genetic research has been hampered by the remote locations of remnant breeding populations and the species’ exceptional wariness in Asia, where it is under hunting pressure. Only one genetic study has directly addressed subspecies delimitations within Asia (Liu et al. 2017), which confirmed currently accepted boundaries and subspecies status. No research thus far has incorporated populations from Central Asia or Mongolia, which are a key bridge between the 2 great bustard subspecies and whose subspecific identity has been variously regarded.

In this work, we aimed to characterize the amount of genetic differentiation between *O. t. tarda* and *O. t. dybowskii*, using the most comprehensive sampling of the Asian great bustard’s range to date. We present novel mitochondrial DNA sequence data from across Central Asia and Mongolia, collected over the course of a decade of field research in remote regions. We analyze these along with archived sequences from Europe to characterize female migration at a broad geographic scale. We use coalescent methods to estimate rates of mitochondrial gene flow between European and Asian bustards and divergence times between the two.

Materials and Methods

Field Collections

We collected great bustard feathers for genetic analyses between 2006 and 2015 (Figure 1A). Specifically, we visited discrete sites in Central Asia and Mongolia at which great bustards gather to breed and stage for migration from within the recognized ranges of both *O. t. tarda* and *O. t. dybowskii* (either west or east of the Altai Mountains, respectively). We collected feathers from *O. t. tarda*

in Almaty, Kostanai, South Kazakhstan, and West Kazakhstan Provinces of Kazakhstan in summer and fall 2006 (collection sites 10–13 in Table 1 and Figure 1). Feathers from *O. t. dybowskii* were collected at sites in Bulgan (site 2), Khentii (site 1), Khövsgöl (sites 3–7), and Uvs (site 8) Provinces of Mongolia during spring, summer, and fall from 2006 through 2015. Most feathers were collected noninvasively, including molted feathers and feathers from dead great bustards (e.g., at sites of poaching and collision with power lines). In 2 cases, feathers from Khövsgöl were collected when great bustards were captured for satellite telemetry research (Kessler et al. 2013). We collected molted feathers from great bustards in Xinjiang, China (site 9) in fall 2015. Collection and transport of these feathers was arranged with compliance to all relevant laws and regulations (CITES permits: Kazakhstan #00KZ001017; Mongolia 2016-#003, 2011-#3468, 2009-#3246, 2007-#3133; extracted DNA rather than whole feathers were exported from China, thus no CITES permit was necessary; USDA Veterinary permits: #52686, #100242, #102223, #105801, #113744, #129386). Feathers were stored dry at room temperature in envelopes, with notes on date, geographic coordinates, number, and sex of birds present.

Laboratory Procedures

A subset of feather samples from sites in Mongolia and Kazakhstan were selected for DNA extraction and sequencing such that all collection sites were represented and the chance that multiple feather samples originated from the same individual was minimized. Because our field site in western China lies closest to the Altai Mountains, the suspected border between subspecies, and because we were interested in determining whether hybridization occurs in the region, we chose more samples from this site. DNA from feathers collected in China was extracted at Junkeyuan Technology Company in Beijing and shipped to the United States for PCR and sequencing. Sequenced samples are listed in Table 1.

Genomic DNA was extracted from feather tissues using Qiagen DNeasy Blood and Tissue Kit (Qiagen, Inc., Germantown, MD) following the user-developed protocol, “Purification of total DNA

from nails, hair, or feathers using the DNeasy Blood & Tissue Kit” (Qiagen, Inc., 2006). For each feather, 2–5 cm of the quill was used including both the inferior and superior umbilicus. DNA was eluted in 100 µL of Buffer AE and stored at –20 °C. DNA quantity was measured using a NanoDrop 2000 spectrophotometer (Thermo Fisher Scientific, Wilmington, DE). We found that samples with 5–10 ng/µL were sufficient for use in polymerase chain reaction (PCR).

We surveyed the literature and GenBank records to identify genes for which the western subspecies of great bustard was well-represented. Based on the results of this survey, we amplified 365 base pairs of the mitochondrial control region (CTR) and 437 base pairs of the mitochondrial cytochrome b (CYTB) gene in our samples using PCR. The CTR region was amplified using the H772 (5′ – AAACACTTGAAACCGTCTCAT – 3′) and L438 (5′ – TCACGTGAAATCAGCAACCC – 3′) primers (Wenink et al. 1993). The CYTB gene was amplified using the Hcyt-B6 (5′ – TCTTTGGTTTACAAGACCAATGTTT – 3′) and Lcyt-B4 (5′ – CCAACCTACTAGGGGACCCAGA – 3′) primers (Broderick et al. 2003).

PCR was completed in 8 µL reactions, including 2 µL of genomic DNA (concentration: 5–10 ng/µL), 1.2 µL reagent-grade DNase-free water, 0.7 µL Q solution (Qiagen), 3.5 µL Qiagen Multiplex Mix (Qiagen), 0.3 µL of each primer (10 µM stock). This resulted in final primer concentrations of 0.375 micromolar, and a final DNA concentration of ~1.5–2.5 ng/µL. Reactions were then subjected to the following PCR protocol: initial denaturing at 95 °C for 15 min; 30–40 cycles of denaturing at 94–95 °C for 30 s, annealing at 51–53 °C for 90 s, and elongation at 72 °C for 1 min; with a final elongation at 60–72 °C for 30 min. PCR products were analyzed by gel electrophoresis in a 1.5% agarose gel to check for successful amplification.

Samples that were successfully amplified were purified using 2 µL of ExoSap-IT (Thermo Fisher Scientific) and 5 µL of PCR product incubated at 37 °C for 30 min and 80 °C for 15 min. PCR products were diluted 10:1, and sequenced in the forward and reverse

Table 1. Summary of great bustard samples used in the analysis, including collection site

Collection site	Population	Region	Subspecies	Sample size	Citation
1	Khentii, Mongolia	Mongolia	<i>dybowskii</i>	2	NA
2	Bulgan, Mongolia	Mongolia	<i>dybowskii</i>	3	NA
3	Khövsgöl, Mongolia	Mongolia	<i>dybowskii</i>	5	NA
4	Khövsgöl, Mongolia	Mongolia	<i>dybowskii</i>	1	NA
5	Khövsgöl, Mongolia	Mongolia	<i>dybowskii</i>	2	NA
6	Khövsgöl, Mongolia	Mongolia	<i>dybowskii</i>	3	NA
7	Khövsgöl, Mongolia	Mongolia	<i>dybowskii</i>	1	NA
8	Uvs, Mongolia	Mongolia	<i>dybowskii</i>	2	NA
9*	Xinjiang, China	Central Asia	<i>tarda</i>	24	NA
10	Almaty Province, Kazakhstan	Central Asia	<i>tarda</i>	2	NA
11	South Kazakhstan Province, Kazakhstan	Central Asia	<i>tarda</i>	3	NA
12	Kostanai Province, Kazakhstan	Central Asia	<i>tarda</i>	2	NA
13	West Kazakhstan Province, Kazakhstan	Central Asia	<i>tarda</i>	1	NA
14	Saratov, Russia	Europe	<i>tarda</i>	8	Pitra et al. (2000)
15	Déaványa, Hungary	Europe	<i>tarda</i>	7	Pitra et al. (2000)
16	Nitra, Slovakia	Europe	<i>tarda</i>	6	Pitra et al. (2000)
17	Rathenow, Germany	Europe	<i>tarda</i>	11	Pitra et al. (2000)
18	Madrid, Spain	Europe	<i>tarda</i>	25	Pitra et al. (2000)
19	Cáceres, Spain	Europe	<i>tarda</i>	9	Pitra et al. (2000)

“Populations” represent the groupings used in the AMOVA. Asterisked sample: mtDNA from one sample at this site grouped with *Otis tarda dybowskii* birds, but was assumed to be part of the *Otis tarda tarda* population in which it was sampled in subsequent analyses. GenBank accessions for each individual as well as citation information and details for outgroup taxa are provided in Supplementary Table S1.

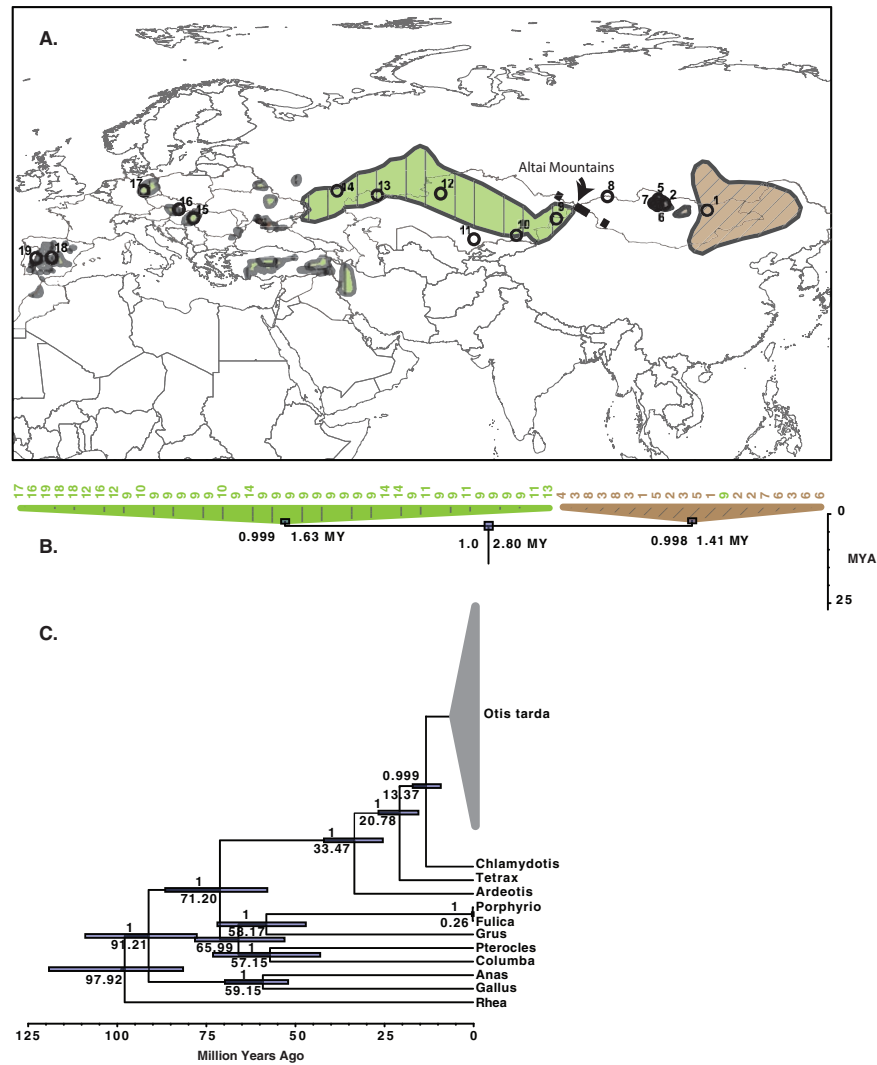


Figure 1. Phylogenetic relationships among mtDNA haplotypes inferred in BEAST v. 1.8.3. **(A)** Sampling locations and species range of *Otis tarda*. Green polygons with vertical stripes represent contemporary range of *Otis tarda tarda*, and brown polygons with diagonal stripes the range of *Otis tarda dybowskii*, as described by BirdLife (2016). Numbers represent locations of samples used in analysis; full locality details are provided in Table 1. Dashed line indicates the location of the Altai Mountains, the presumed boundary between the 2 subspecies. **(B, C)** Maximum clade credibility trees show relationships among *O. tarda* haplotypes **(B)**, and among outgroup sequences used to calibrate rates of sequence evolution **(C)**, as well as the times to common ancestry between clades. Clade posterior probabilities are shown to the left of each node (in **B**), or above the node (in **C**), node ages are shown to the right (in **B**), or below each node (in **C**). Error bars on nodes show the 95% highest posterior density intervals. For simplicity of presentation, some relationships within *O. tarda* are collapsed. A fully resolved consensus tree is available in Supplementary Figure 1. See online version for full colors.

directions using Sanger sequencing with dye-terminators by the DNA Laboratory at Arizona State University. Sequencing reactions were analyzed by capillary electrophoresis on an Applied Biosystems 3730XL Sequence Analysis Instrument (Thermo Fisher Scientific).

Electropherograms were inspected, and sequence data were edited using CodonCode Aligner Version 3.7.1.2 (CodonCode Corp. Centerville, MA). Low-quality sequences and sequence ends were automatically discarded using the Clip Ends tool in CodonCode. Forward and reverse reads from each individual were built into contigs, and contigs were aligned against each other to create “contigs of contigs” using the built-in assembly algorithm in CodonCode. The quality of the electropherogram data underlying every putative mutation identified in the contig of contigs was checked by eye by 2 independent observers. Edited sequence data from each individual were exported as separate FASTA files. Sequences have been deposited in GenBank (accession numbers available in Supplementary Table S1).

Sequence Alignment and Data Description

We obtained CTR and CYTB sequences from European populations of great bustard and outgroup taxa from GenBank (Tables 1 and 2). Outgroup taxa were selected to capture diversity within birds and maximize the number of potential calibration points based on records described in Prum et al. (2015) and Jarvis et al. (2014). Sequences were aligned using Clustal Omega v. 1.2.2 through the European Bioinformatics Institute’s web submission portal. Finally, aligned sequences were imported into Mesquite v. 3.0.5 build 725, and the terminal ends of the alignments were trimmed to remove large sections of missing data.

Our final dataset included new sequence data from 53 feather samples, consisting of 8 samples from 4 sites in Kazakhstan (sites 10–13), 20 samples from 8 sites in Mongolia (sites 1–8), and 24 samples from 1 site in western China (site 9). In 5 samples either the CYTB or CTR regions failed to amplify. These samples were

excluded from further analyses, leaving 51 individuals with data from both regions. From GenBank, we obtained matched CYTB and CTR sequences from 66 individuals from Europe (Germany, Hungary, Russia, Spain, and Slovakia; sites 14–19). Finally, we obtained both CTR and CYTB data for 11 outgroups, including *Anas crecca* (Anatidae), *Ardeotis kori* (Otididae), *Chlamydotis undulata* (Otididae), *Columba livia* (Columbidae), *Fulica atra* (Rallidae), *Gallus gallus* (Phasianidae), *Grus rubicunda* (Gruidae), *Porphyrio porphyrio* (Rallidae), *Pterocles namaqua* (Pteroclididae), *Rhea americana* (Rheidae), and *Tetrax tetrax* (Otididae).

Phylogenetic Analysis

To infer rates of sequence evolution in the 2 mitochondrial regions, and to estimate relationships among mitochondrial haplotypes within *O. tarda*, we completed phylogenetic analyses of the complete dataset (including all outgroups). We selected models of sequence evolution using jModelTest2 (Darriba et al. 2012) running on the jmodeltest.org servers. We selected models for CYTB and CTR separately, using an Akaike information criterion to select an optimal model while preventing over-fitting. This procedure selected a TrN+I+G model for CYTB and an HKY+G model for CTR.

To test for a molecular clock, we used likelihood ratio tests to compare the best-fit model selected by jModelTest2 with a model enforcing a molecular clock but keeping all other parameters the same. We calculated likelihood scores in PAUP* v. 3.0B 10 (Swofford 2002), on trees inferred using neighbor-joining, rooting the trees with *Rhea americana* and constraining the ingroup to be monophyletic. A molecular clock could not be rejected for either dataset (likelihood ratio test, df = 69; CTR LR = 74.62, $P = 0.30$; CYTB LR = 57.18, $P = 0.84$).

We estimated phylogenetic relationships, divergence times, and mutation rates jointly using BEAST v. 1.8.3 (Drummond et al. 2012). We used BEAUti v. 1.8.3 to create input files for BEAST. To allow different substitution models and mutation rates between gene regions, we loaded the CTR and CYTB separately in BEAUti, linking the tree models, but allowing the substitution and molecular clock models to remain unlinked. We specified a Yule model for the tree prior and initialized the Markov Chain Monte Carlo with a random starting tree. For each gene region, we specified the family of substitution models and rate heterogeneity (TrN+I+G and HKY+G, respectively) but allowed BEAST to estimate the base frequencies and the transition rate parameters. To aid in the estimation of divergence times and mutation rates, we defined 4 different taxon sets. The taxon sets were as follows: the Neognathae (all taxa except *Rhea americana*), the Gruiformes (*Fulica atra*, *Grus rubicunda*, and *Porphyrio porphyrio*), *Pterocles* + *Columba*, and *Anas* + *Gallus*. Each taxon set was constrained to be monophyletic, and for each, we defined a prior age distribution following Jarvis et al. (2014) and Prum et al. (2015). In each case, we specified a log-normal prior, offset from zero based on relevant fossil calibrations, and

specifying means and standard deviations so that the median of the prior distribution would match the posterior age estimates in Jarvis et al. (2014). Full prior parameters for each age calibration are listed in Table 2. Finally, following Pereira et al. (2004), we specified lognormal prior distributions on the substitution rates for CYTB and CTR each means of 3.23×10^{-3} S/S/MY and 1.6×10^{-3} S/S/MY, respectively, and a log standard deviation of 1.0 in both cases.

We completed 2 independent Markov Chain Monte Carlo (MCMC) simulations in BEAST, each 10 million generations long, and each with a 100 000 generation burn-in. To assess stationarity, we examined trends in the likelihood scores and parameter estimates across the MCMC using Tracer v. 1.6.0 (Rambaut and Drummond 2003). To assess convergence, we examined the effective sample sizes, and compared parameter estimates and their distributions between independent runs in Tracer. Mutation rates were estimated from the combined output from both runs. Post-burn-in trees from both runs were combined using the LogCombiner program and summarized using the TreeAnnotator program (both programs are distributed with the BEAST package). Finally, the consensus tree was visualized using FigTree v. 1.4.3 (Rambaut 2009).

Population Genetic Analyses

Although our primary goal was to characterize genetic differentiation between the Asian and European populations, we also calculated summary statistics describing genetic variation. To compare genetic diversity between sites and between regions, we used DNAsp v 5 (Librado and Rozas 2009) to calculate the number of haplotypes, the number of segregating sites (S), haplotype diversity (Hd), the average number of pairwise differences between sequences (k), and the per-site population mutation rate (θ) under a finite sites model (Tajima 1996). (Population groupings for calculating these summary statistics were as shown in Table 1.)

To further visualize the geographic distribution of genetic variation, we collapsed our sequences into haplotypes and computed a minimum spanning network (Bandelt et al. 1999) in popart v. 1.7 (Leigh and Bryant 2015). We then counted the number of the copies of each haplotype found in each population and calculated the proportion of copies found in each.

To quantify mitochondrial geographic structure within and between subspecies we completed analyses of molecular variance (AMOVAs) in Arlequin v. 3.5 (Excoffier 2010). First, we analyzed the complete *O. tarda* dataset, partitioning genetic variation into the fractions between subspecies, the fraction between populations within subspecies, and the fraction within populations. Next, we analyzed sequences from *O. t. tarda* alone, partitioning genetic variation into the fractions between Europe and Central Asia, the fraction between populations within regions, and the fraction within populations (again, population and regional groupings were as shown in Table 1). We used permutation tests implemented in

Table 2. Posterior and prior distributions of key node ages in the BEAST analysis

Clade	Fossil age (MY)	Citation	Prior				Posterior		
			Mean	SD	Offset	Median	Mean	SD	95% HPD
Gruiformes	28.4	Mayr (2005)	40	0.5	28.4	63.6	58.6	6.46	47.09–71.79
Neognathae	66–70	Noriega and Tambussi (1995)	25	0.5	66	88.06	92.08	8.27	77.69–108.89
<i>Pterocles</i> + <i>Columba</i>	18	Becker et al. (1992)	50	0.5	18	62.12	57.56	7.7	43.16–73.15
<i>Anas</i> + <i>Gallus</i>	50.3	Olson (1999)	20	0.75	50.3	65.4	59.89	4.94	51.83–69.51

SD, standard deviation.

Arlequin to determine whether variance components were statistically significant.

To estimate population genetic parameters, we analyzed sequence data using IMA v. 2.0 (Hey 2010). Because IMA does not allow missing data, we trimmed the dataset to include only sites present in all samples. The resulting, trimmed dataset was 586 bp in length, including 297 bp from CYTB and 289 bp from CTR. Because the AMOVA results (below) suggested that a significant fraction of genetic variation is distributed between subspecies, but not between European and Central Asian (Kazakhstani and Chinese) populations of *O. t. tarda*, we grouped the sequence data into just 2 populations representing *O. t. tarda* and *O. t. dybowskii*.

To determine prior distributions for parameters to be estimated, we calculated the average pairwise differences between sequences within *O. t. tarda* and *O. t. dybowskii* and then used the larger of these 2 values as an initial estimate of the population mutation rate (θ). We then set priors on θ , t (the time to divergence between *O. t. tarda* and *O. t. dybowskii*) and m (the per-individual migration rate scaled relative to the per-locus mutation rate), based on the recommendations in the IMA manual. To allow the data to trump these hard priors, we adjusted the prior settings dynamically based on initial analyses. (For example, if the parameter value with the highest posterior probability for θ was equal to the maximum value allowed based on the prior, we considered that to be an indication that our prior value was too low, and re-ran the analysis using a higher prior). The priors used in the final analysis were as follows: $\theta = 16$, $t = 10$, $m = 5$.

We set IMA to estimate the asymmetric migration rates between extant populations only and allowed population sizes in the ancestral and descendant populations to vary independently. We set the program to print the distribution of the population migration rate (2NM) and assumed a generation time of 4 years, based on evidence that great bustards typically first breed at 3–5 years of age (Lane and Alonso 2001). We used a 1 million generation MCMC, with a 10000 generation burn-in. We completed 2 independent MCMCs, and compared parameter estimates between runs. To assess convergence, we compared the posterior probabilities for values of each estimated parameter and measured correlation in posterior probabilities between runs. Across all parameters, posterior probabilities

were more than 99% correlated between runs. Final parameter estimates were averaged across the 2 runs.

In addition, at the suggestion of an anonymous reviewer, we analyzed the CYTB and CTR partitions separately to evaluate how differences in mutational processes between these 2 genes impacted estimated parameters. All search settings and prior distributions were as described above for the complete dataset.

Results

Phylogeny estimation using BEAST found strong support (>99% posterior probability) for the monophyly of the Otididae, with *O. tarda* being more closely related to the houbara bustard (*C. undulata*) than to the kori bustard (*A. kori*) or the little bustard (*T. tetrax*) (Figure 1C). There was also very strong support for the monophyly of *O. tarda* s. l., with the common ancestor of all extant mtDNA sequences having lived approximately 2.8 million years ago (highest posterior density [HPD] = 1.66–3.88 million years). Within *O. tarda* there was strong support for 2 clades, one representing exclusively individuals of *O. t. tarda* from Europe, Kazakhstan, and Xinjiang (sites 9–19), and the second representing all individuals of *O. t. dybowskii* from Mongolia (sites 1–8), plus 1 individual collected in Xinjiang (site 9). For simplicity of presentation, we have collapsed these clades in Figure 1C. The fully resolved consensus tree is available in Supplementary Figure 1. Relationships within each of these 2 major clades were generally very weakly supported (<<50% posterior probability). Exceptions included a clade composed of 3 samples from Khövsgöl, Mongolia (sites 3 and 6; 99% posterior probability) and a clade composed of 3 samples from Xinjiang, China (site 9; 100% posterior probability). In both cases, these represent geographically restricted, distinct haplotypes. BEAST inferred a substitution rate of $2.78 \times 10^{-3} \pm 7.49 \times 10^{-6}$ S/S/MY (HPD = 1.97×10^{-3} to 3.66×10^{-3}) for the CYTB region. For the CTR region BEAST inferred a substitution rate of $4.64 \times 10^{-3} \pm 5.36 \times 10^{-6}$ S/S/MY (HPD = 3.68×10^{-3} to 5.62×10^{-3}).

Popart identified 14 haplotypes, including 4 common haplotypes with broad geographic distributions and 10 that were unique to particular localities (Table 3). Diversity statistics in each population and in each region are shown in Table 4. Many populations were fixed

Table 3. Haplotype distribution for samples of *Otis tarda* by sampling location

Population	Haplotype number													
	1	2	3	4	5	6	7	8	9	10	11	12	13	14
Khentii, Mongolia	—	—	—	—	—	—	—	—	—	—	—	2	—	—
Bulgan, Mongolia	—	—	—	—	—	—	—	—	—	1	—	1	—	1
Khövsgöl, Mongolia	—	—	—	—	—	—	—	—	—	—	1	8	3	—
Uvs, Mongolia	—	—	—	—	—	—	—	—	—	—	—	2	—	—
Xinjiang, China	—	—	—	19	—	3	—	—	1	—	—	1	—	—
Almaty Province, Kazakhstan	—	—	—	2	—	—	—	—	—	—	—	—	—	—
South Kazakhstan	—	—	1	2	—	—	—	—	—	—	—	—	—	—
Kostanai, Kazakhstan	—	—	—	2	—	—	—	—	—	—	—	—	—	—
West Kazakhstan	—	—	—	—	—	—	—	1	—	—	—	—	—	—
Saratov, Russia	5	—	—	3	—	—	—	—	—	—	—	—	—	—
Déaványa, Hungary	5	2	—	—	—	—	—	—	—	—	—	—	—	—
Nitra, Slovakia	4	—	—	2	—	—	—	—	—	—	—	—	—	—
Rathenow, Germany	11	—	—	—	—	—	—	—	—	—	—	—	—	—
Madrid, Spain	5	4	—	—	—	—	16	—	—	—	—	—	—	—
Cáceres, Spain	4	2	—	—	3	—	—	—	—	—	—	—	—	—

Haplotype numbers match those shown in Figure 2. Numbers in each cell show the number of copies of each haplotype found in each population.

Table 4. Summary statistics showing measures of genetic diversity in each region and each population

	Haplotypes	Segregating sites	Haplotype diversity	Average pairwise differences	Theta
Region					
Mongolia	5	4	0.526	0.690	0.00118
Central Asia	6	9	0.389	1.014	0.00173
Europe	5	4	0.663	1.476	0.00253
Population					
Mongolia: Bulgan	3	2	1	1.333	0.00228
Mongolia Khentii	1	0	0	0	—
Mongolia: Khövsgöl	3	3	0.53	0.742	0.00127
Mongolia: Uvs	1	0	0	0	0
Central Asia: Xinjiang	4	9	0.370	1.192	0.00204
Central Asia: Almaty	1	0	0	0	—
Central Asia: NW Kazakhstan	1	0	0	0	—
Central Asia: S Kazakhstan	2	1	0.667	0.667	0.00114
Europe: Cáceres, Spain	3	3	0.722	1.389	0.00238
Europe: Hungary	2	1	0.476	0.476	0.00081
Europe: Madrid, Spain	3	4	0.547	1.720	0.00295
Europe: Russia	2	1	0.536	0.536	0.00092
Europe: Slovakia	2	1	0.533	0.533	0.00091

for a single haplotype, with a maximum of 3 haplotypes per population. Despite typically low levels of genetic variation overall, and despite smaller sample sizes in this study, the genetic diversity statistics for Asian populations (sites 1–13) were comparable to populations in Europe (sites 10–19), with roughly equal numbers of haplotypes per population, segregating sites, and haplotype diversity. Consistent with the BEAST analysis, the minimum spanning network identified 2 clades (Figure 2), separated by a long internal branch, representing birds from Europe, Kazakhstan, and western China (sites 9–19) on the one hand and birds from Mongolia (sites 1–8), and one individual from western China (site 9) on the other.

The results of AMOVA are shown in Tables 5 and 6. The AMOVA comparing *O. t. tarda* with *O. t. dybowskii* revealed that 79.90% of variation is distributed between subspecies, and the subspecies effects are strongly statistically significant ($P < 0.0001$). Meanwhile, much smaller, but statistically significant, fractions of variation were distributed between populations within subspecies (7.12%, $P < 0.001$) and within populations (12.98%, $P < 0.001$). In contrast, the AMOVA comparing Central Asian (sites 9–13) and European populations (sites 14–19) within *O. t. tarda* revealed that only 19.44% of variation was distributed between regions, and this effect was only weakly statistically significant ($P = 0.024$). As in the comparison between subspecies, there was a significant effect of population within regions ($P < 0.001$), explaining 23.97% of variation in *O. t. tarda*, and a significant fraction of the variation (56.59%, $P < 0.001$), was found within populations.

Coalescent analyses of the concatenated dataset using IMA suggest that *O. t. tarda* and *O. t. dybowskii* diverged from a common ancestral population approximately 1.4 million years ago (Figure 3), and have been relatively genetically isolated (with respect to the mitochondrial genome) since then, exchanging less than 1 female migrant per generation. Coalescent estimates of migration suggest a per-generation migration rate of 0.503 female migrants moving from *O. t. dybowskii* into *O. t. tarda* and effectively zero migration from *O. t. tarda* into *O. t. dybowskii*; the migration rate with the highest posterior probability (0.02) was the lowest value considered, as IMA does not actually estimate the probability of zero migrants (Figure 4).

Analyses of the CYTB and CTR datasets alone inferred similar rates of female gene flow (CYTB: 0.472 female migrants per generation from *O. t. dybowskii* into *O. t. tarda*, 0.02 female migrants from *O. t. tarda* into *O. t. dybowskii*; CTR: 1.619 female migrants per generation from *O. t. dybowskii* into *O. t. tarda*, 0.02 female migrants from *O. t. tarda* into *O. t. dybowskii*). However, analyses of the separate datasets suggest slightly lower divergence times than were inferred from the concatenated data (CYTB: 932 thousand years ago, CTR: 562 thousand years ago). We suspect the reason for the younger ages is that there is a fair amount of homoplasy in CTR region within the European bustards. (This homoplasy is evident in the reticulate haplotype network shown in Figure 2.) However, the convergent nature of the mutations in the control region is only evident when analyzing the concatenated dataset; without the CYTB data these homoplasies appear to be homologies, and the degree of sequence divergence is therefore underestimated.

Discussion

Our results strongly suggest that *O. t. tarda* and *O. t. dybowskii* have been genetically isolated from one another for an extended period of time, at least when considering the mitochondrial genome. Phylogenetic analysis, analyses of molecular variation, and coalescent estimation of divergence times and migration rates all suggest high levels of genetic differentiation in the mitochondrion between the 2 subspecies, and a long history of isolation. The distribution of mitochondrial haplotypes alone provides strong evidence for genetic differentiation between *O. t. tarda* and *O. t. dybowskii*. Almost all haplotypes were found only in 1 of the 2 subspecies, though a single individual from Xinjiang, on the eastern edge of the range of *O. t. tarda* (Figure 1, site 9), carried a mitochondrial haplotype typical of *O. t. dybowskii*. Liu et al. (2007) previously analyzed great bustard mtDNA collected within China and found that *O. t. dybowskii* was monophyletic, nested within a paraphyletic *O. t. tarda*. Strikingly, they also identified 1 “misplaced” sequence from Xinjiang that falls as sister to *O. t. dybowskii*. No observations of *O. t. dybowskii* have been recorded in Xinjiang or adjacent eastern Kazakhstan (Berezovikov 1986; BirdLife International 2001)

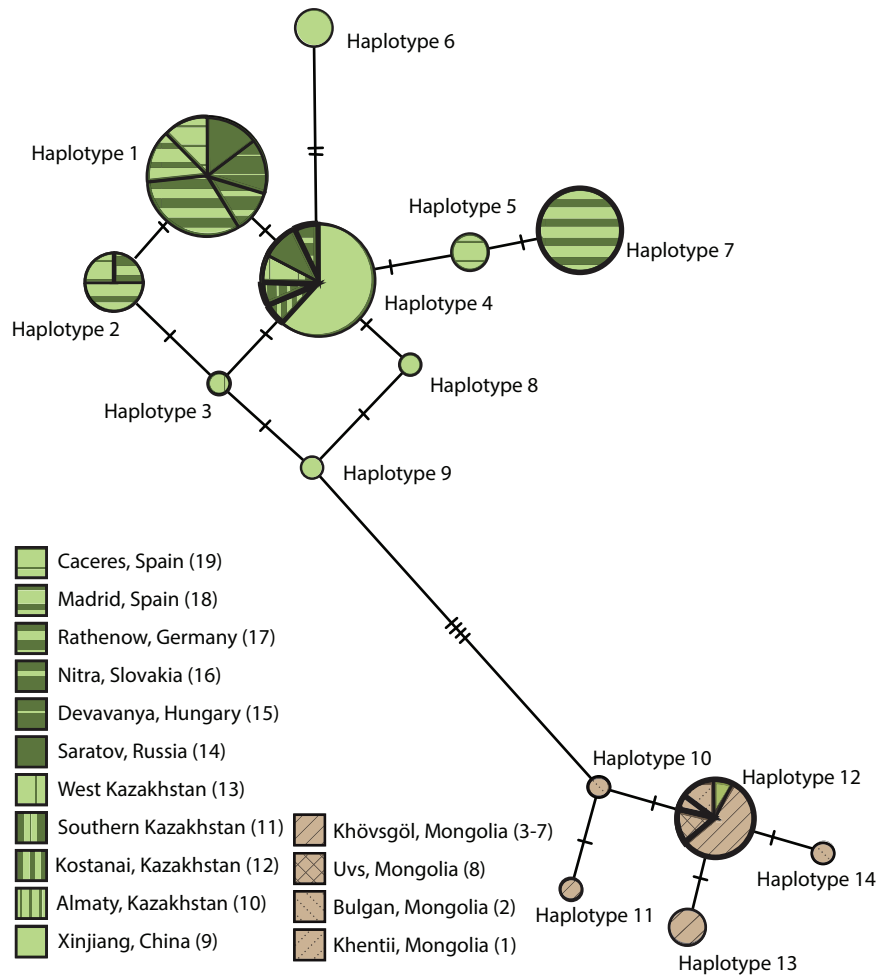


Figure 2. Minimum spanning network showing relationships among haplotypes within *Otis tarda* inferred in popart v. 1.7. The size of each circle is proportional to the number of copies of each haplotype. Mutational differences between each haplotype are shown as hash marks along each edge; edges with no hash marks show haplotypes separated by one mutation. Patterns and colors represent sampling location (see legend in lower left), with shades of green and vertical or horizontal stripes representing locations in Europe and Central Asia (*Otis tarda tarda*) and shades of brown with diagonal stripes representing locations in Mongolia (*Otis tarda dybowskii*). See online version for full colors.

Table 5. AMOVA comparing variation within and between subspecies (*Otis tarda tarda* vs. *Otis tarda dybowskii*)

Source	df	Sum of squares	Variance component	Percent variation
Between subspecies	1	100.024	3.04407	79.90
Between populations within subspecies	11	30.501	0.27140	7.12
Within populations	104	51.424	0.49446	12.98
Total	116	181.949	3.8093	

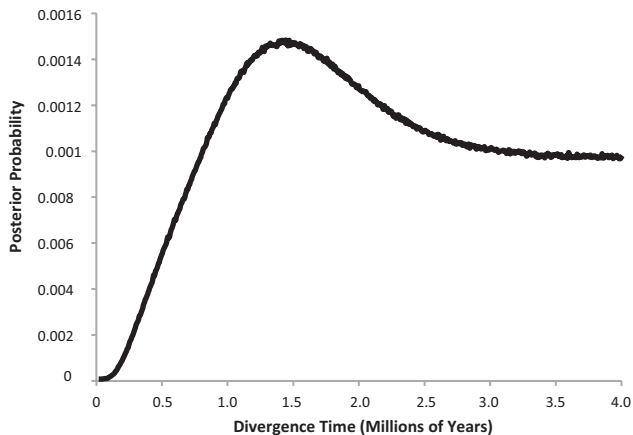
and the closest populations of *O. t. dybowskii* have been extirpated (Irisova 2008). It is unclear whether the unexpected phylogenetic placement of our sample reflects historic gene flow, retention of ancestral polymorphisms, or recent dispersal, but the similarity between our results and Liu's previous work (2007) suggests that Xinjiang may have been a region of hybridization or secondary contact between the 2 groups.

The coalescent analyses implemented in IMA also strongly argue for genetic isolation in the mitochondrial genome between the 2 subspecies. The divergence time estimates suggest a long history of isolation, with the 2 subspecies having diverged at least 1 million years ago. Our estimates of the asymmetric female migration rates suggest extremely low levels of gene flow between *O. t. tarda*

and *O. t. dybowskii*, which reinforces a picture of genetic isolation between the 2 subspecies. Estimated rates of mitochondrial gene flow from *O. t. tarda* into *O. t. dybowskii* were not statistically different from zero (the smallest possible parameter value has the highest posterior probability). Although mitochondrial gene flow from *O. t. dybowskii* into *O. t. tarda* was noticeably greater than zero (likely due to the "misplaced" mitochondrial haplotype discussed above), it is still low enough to be consistent with a history of genetic isolation. Wright (1931) showed analytically that populations begin to diverge through genetic drift alone when they exchange less than 1 migrant per generation, though divergent natural selection can maintain differences even in the face of much higher levels of gene flow. Rates of mitochondrial gene flow between *O. t. dybowskii* and

Table 6. AMOVA comparing variation between regions within *Otis tarda tarda* (Europe vs. Central Asia)

Source	df	Sum of squares	Variance component	Percent variation
Between regions	1	12.041	0.17761	19.44
Between populations within regions	7	17.666	0.21898	23.97
Within populations	89	46.007	0.51694	56.59
Total	97	75.714	0.91353	

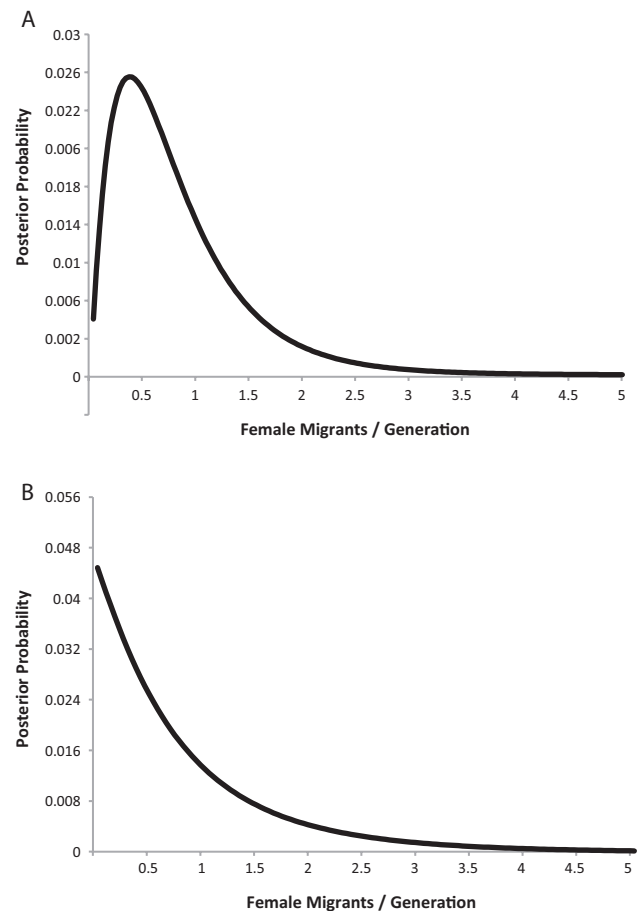
**Figure 3.** Divergence time between *Otis tarda tarda* and *Otis tarda dybowskii* inferred in IMA2 v. 8.27.12. The x axis shows the range of parameters (divergence times) considered, and the y axis shows the posterior probability of each age estimate. The age with the highest posterior probability is 1.401 million years ago.

O. t. tarda as estimated from the combined CYTB and CTR data are much less than 1 migrant per generation.

Our study includes only data from the mitochondrial genome, which is maternally inherited. Female great bustards in Spain have been described as highly philopatric with males as the dispersing sex (Martín et al. 2002, 2008). If this trait is consistent across the species' range, our data may exaggerate the degree of genetic isolation between the 2 subspecies. Yet, our finding of a rather small fraction of genetic variation distributed between Central Asia and Europe within *O. t. tarda*, and an extremely wide geographic distribution of haplotypes within *O. t. tarda*, indicate extensive female movement. Indeed, a study of gene flow in the Ponto-Caspian Basin found that female great bustards exhibited a high dispersal rate over evolutionary time (Pitra et al. 2007). Female dispersal may be more prevalent in the east of the species' range, where females carry out long-distance migratory movements (Oparina et al. 2001; Zav'yalov et al. 2003; Kessler et al. 2013). Given the signature of female movement we observe within *O. t. tarda*, it seems unlikely that the extent of the differences we observe between the subspecies could be attributed to female philopatry alone. Nonetheless, given the limitations of analyses based on mitochondrial data alone, our findings should be viewed as provisional, and future work should incorporate data from nuclear markers in order to obtain a picture of subspecies isolation and regional genetic structure that also captures male dispersal.

Implications for Taxonomic Status

Our results are consistent with, but do not definitively prove, the proposition that *O. t. dybowskii* and *O. t. tarda* are distinct species. The distribution of haplotypes, phylogenetic analysis, AMOVAs, and

**Figure 4.** Coalescent estimates of female migration rates (i.e., migrants per generation) (A) from *Otis tarda dybowskii* into *Otis tarda tarda* and (B) from *O. t. tarda* into *O. t. dybowskii* inferred in IMA2 v. 8.27.12. The x axis shows range of migration rates considered, the y axis shows the posterior probability of each rate estimate. In panel "A," the migration rate with the highest posterior probability is 0.503. In panel "B," the migration rate with the highest posterior probability is 0.020 female migrants (i.e., the smallest value considered).

coalescent estimates of female migration rates and divergence time indicate that the subspecies are highly genetically differentiated in their mitochondrial genomes and have been genetically isolated for approximately 1.4 million years. This is 3 times longer than the time since differentiation of the taxa most closely related to the great bustard, the houbara bustard (*C. undulata*) and Asian houbara bustard (*Chlamydotis macqueenii*), which are now widely accepted as 2 species (Idaghdour et al. 2004).

The only other study to directly address genetic differentiation between great bustard subspecies examined variation in the mitochondrial control region from several populations of *O. t. dybowskii*

from northeastern China (Liu et al. 2017). Their results were similar to the findings we present here (i.e., that *O. t. tarda* and *O. t. dybowskii* are 2 genetically distinct groups), but Liu et al. (2017) concluded that the levels of sequence divergence between them were too low to classify *O. t. dybowskii* as a distinct species. We disagree with this interpretation of the data for 2 reasons.

First, the standard used by Liu et al. (2017) to distinguish species from subspecies could be improved. The amount of sequence divergence within and between species varies widely depending on the gene regions used and the taxa under consideration. In this case, the standard that Liu et al. (2017) used to delimit species versus subspecies (6% sequence divergence) is based on a literature review of non-avian reptile studies (Torstrom et al. 2014), represents the average sequence divergence between subspecies elevated to species status, and was based on both nuclear and mitochondrial genes. If we apply a more appropriate benchmark, the levels of sequence divergence between *O. t. tarda* and *O. t. dybowskii* are consistent with them being separate species. Hebert et al. (2004) calculated the average percent sequence divergence in the mitochondrial gene cytochrome oxidase one (COI) both within and between species in 260 birds. They found that the average sequence divergence between conspecific individuals was 0.43%, with a maximum sequence divergence of 1.24%. Based on our CYTB data alone, we calculated an average of 1.4% sequence divergence between *O. t. tarda* and *O. t. dybowskii*. However, the rate of sequence evolution in COI is ~2.4 times faster than CYTB [cf. Tables S4 and S7 in Pereira and Baker (2006)]. Adjusting for these relative mutation rates, the sequence divergence we see in CYTB is equivalent to ~3.5% divergence in COI, or more than 8 times the sequence divergence typically seen within bird species and roughly 3 times the maximum sequence divergence in intra-specific comparisons. Thus, if we were to make an evaluation based on sequence divergence in the mitochondrial genome, *O. t. tarda* and *O. t. dybowskii* should be classified as distinct species.

Second, we believe that distance measures alone are not the best criterion by which to determine species status. Species delimitation based on sequence divergence can be useful in some applications, for example, in DNA barcoding studies or when working with rare species represented by a single specimen (Lim et al. 2012). However, in cases where large amounts of sequence data are available from many individuals, methods that consider the underlying population genetic processes involved (gene flow, genetic drift, and reproductive isolation) are preferable. Such methods might include clustering algorithms that group individuals into populations by minimizing departures from Hardy–Weinberg equilibrium (e.g., Pritchard et al. 2000), multispecies coalescent models that seek to identify the transition point between the coalescence of alleles within species and divergence between species (Pons et al. 2006), or the estimation of population genetic parameters as we have done here. Last, inferences based on multiple independent markers will always be stronger than those based on a single, nonrecombining, uniparentally inherited marker such as the mitochondrion.

Ultimately, genetic data should be supplemented with organismal studies of ecology, behavior, and morphology that can identify isolating mechanisms. In the case of great bustard subspecies, comparison of plumage used in courtship may be useful in the evaluation of the potential of interbreeding. The great bustard performs an elaborate visual display, in which white plumage plays a key role (Olea et al. 2010). The color white is particularly effective at signaling in conditions of low light (Penteriani and Delgado 2017), such as dawn and dusk when great bustards display most actively (Hidalgo de Trucios

and Carranza 1991; Zhao 2002). Great bustard subspecies differ in the extent of white plumage on the wing and the tail. There is also a difference in placement of plumes near the bill that are displayed prominently during the breeding display, and the length of which is considered an indicator of male body condition and status (Morales et al. 2003; Alonso et al. 2010). It is possible that these differences in sexual characteristics serve an interspecific isolating function. A comparison of the structure of the display of *O. t. tarda* and *O. t. dybowskii* could also yield information useful to taxonomic decision-making.

Genetic Diversity

Summary statistics of genetic diversity suggest comparable levels of genetic diversity within Central and Inner Asia and in Europe. Differences in genetic diversity estimates between populations may be attributable to differences in the collection procedures between sites and between studies (e.g., whether multiple leks were included in a single population, how many individuals were sampled, etc.). However, both the geographic distributions of haplotypes (Table 3 and Figure 2) and the population genetic summary statistics (Table 4) suggest high levels of genetic diversity in Mongolia (sites 1–8) and Xinjiang (site 9). In particular, northern Mongolia (Bulgan and Khövsgöl Provinces, sites 2–7) contained high haplotype diversity, including 2 haplotypes found only in Bulgan (site 2) and 2 found only in Khövsgöl (sites 3–7). Likewise, Xinjiang, China (site 9) appears to be particularly unusual. This region exhibits high haplotype diversity, containing more haplotypes and a higher number of segregating sites than any other population in either Asia or Europe. In addition, this is the only site that contained genotypes from both of the 2 deeply diverged mitochondrial clades identified here. Future work should focus on this region to evaluate whether the 2 subspecies occur in sympatry here and whether there is greater evidence for either hybridization or historic gene flow.

Conservation Implications

Our findings that *O. t. tarda* and *O. t. dybowskii* exchange much less than 1 female migrant per generation indicates that they should be managed as separate evolutionary units (sensu Moritz 1994). Our findings also indicate that the disappearance of Central Asian and Mongolian great bustards would result in the loss of a valuable reservoir of genetic variation. Urgent measures are required to protect the remaining populations of both *O. t. tarda* and *O. t. dybowskii* in Asia, where populations of both subspecies are critically small, declining, and often isolated by hundreds of kilometers.

The population of *O. t. tarda* in Central Asia is likely less than 500 individuals (Kessler 2016), and the extreme distances between many of the remaining breeding populations in this region today are likely to result in reduced gene flow. Our work indicates that populations breeding in Kazakhstan and Europe are moderately differentiated in mitochondrial DNA, though further research is necessary to determine whether the subspecies label *O. t. korejewi* should be reapplied. In addition, the presence of private alleles in northwest Kazakhstan (site 13), and in Xinjiang (site 9), suggest some mitochondrial geographic structure across Central Asia, although small sample sizes limit our ability to evaluate this statistically. Future work with rapidly evolving nuclear markers, such as microsatellite markers, which better capture recent changes in population

structure, should examine the extent to which these sites experience inbreeding due to drastic population declines in the 20th century, and provide guidance for conservation measures to maintain gene flow. As described above, Xinjiang (site 9), the eastern terminus of the range of the subspecies, emerged as a site of high genetic diversity. Sites in Xinjiang and adjacent East Kazakhstan Province, which almost certainly intermix, should be given particular priority for protection to prevent inbreeding depression and maximize the potential for future adaptation.

Conservation programs in range states of *O. t. dybowskii* should recognize the highly threatened status of this form. Approximately 1500 individuals of the Asian great bustard remain across the 2000 km east-west range in which these birds are still observed. Limited mitochondrial geographic structure was observed in Mongolia. Khövsgöl (sites 3–7) and Bulgan (site 2) Provinces contained the highest levels of genetic diversity and unique haplotypes and should be prioritized in conservation efforts.

Supplementary Material

Supplementary data are available at *Journal of Heredity* online.

Funding

Funding for fieldwork was provided by National Geographic (grant #WW-041C-17), The Mohamed bin Zayed Species Conservation Fund (project #0925616), The Disney Worldwide Conservation Fund, The Rufford Small Grants for Nature Conservation (reference #20.10.07 & 8538-2), a grant from the US National Science Foundation to O. Jensen (Award #1064843), The Ornithological Society of the Middle East, the Caucasus, and Central Asia, The Cleveland Metroparks Zoo, The Melikian Center, The Arizona State University Graduate Student Association, The American Museum of Natural History Frank M. Chapman Memorial Fund, a grant from National Natural Science Foundation of China (grant #31401988), donations from a member of the Great Bustard Group and 100 members of the public via RocketHub crowdfunding. Nigel Collar contributed funds toward permitting for feather export. Celestron Incorporated and National Wild Turkey Foundation provided equipment used in field research. The Willamette University Biology Department provided funding to support laboratory work as part of Malia Santos's senior thesis. A.E.K. was supported by a US National Science Foundation Graduate Research Fellowship, The Wildlife Conservation Society Graduate Research Fellowship, The US National Security Education Program Boren Graduate Fellowship, The P.E.O. Scholar Award, IREX Individual Advanced Research Opportunities Fellowship, The Lisa Dent Memorial Fellowship, and the School of Life Sciences at Arizona State University.

Acknowledgments

We thank The Association for the Conservation of Biodiversity of Kazakhstan, The Taimen Conservation Fund, The Wildlife Science and Conservation Center of Mongolia, Oleg Belyalov, Evgenii and Tatyana Bragin, Enkhtuyaa Dorjkhüü, Erdenetsetseg Dorjkhüü, Dorjkhürel Dulamsüren, Boris Gubin, Todd Katzner, Ainur Shakenova, Andrew Smith, Pürevdorj Sürenkhorloo, and Dana Zhandaeva for logistical support and assistance with fieldwork. Emily Abraham, Jacob Munsen McGee, and Andrea Saunders assisted with the initial development of laboratory protocols. We thank Nigel Collar and Matthew Toomey for comments on the manuscript.

Data Availability

We have deposited the primary data underlying these analyses as follows:

- DNA sequences: GenBank accessions are listed in [Supplementary Table S1](#): MH306089–MH306140 and MH306141–MH306192
- Sampling locations are provided in [Table 1](#)

References

- Alonso JA, Alonso JC, Magaña M, Palacín CA, Martín CA, Martín B. 2009. The most extreme sexual size dimorphism among birds: allometry, selection, and early juvenile development in the great bustard (*Otis tarda*). *Auk*. 126:657–665.
- Alonso JC, Magaña M, Martín CA, Palacín CA. 2010. Sexual traits as quality indicators in lekking male great bustards. *Ethology*. 116:1084–1098.
- Alonso JC, Palacín CA. 2010. The world status and population trends of the great bustard (*Otis tarda*): 2010 update. *Chin Birds*. 1:141–147.
- Bandelt HJ, Forster P, Röhl A. 1999. Median-joining networks for inferring intraspecific phylogenies. *Mol Biol Evol*. 16:37–48.
- Becker JJ, Brodtkorb P, Campbell KE Jr. 1992. An early Miocene ground dove (Aves: Columbidae) from Florida. *Pap Avian Paleontol Honor Pierce Brodtkorb Nat Hist Museum Los Angeles County Sci Ser*. 36:189–193.
- Berezovikov NN. 1986. Contemporary status of the great bustard in Eastern Kazakhstan. In: Gabuzov OS, editor. *Bustards and methods of their conservation: a scientific handbook*. Kalinin (USSR): TsNIL Glavokhoty. p. 48–52. In Russian.
- BirdLife International. 2001. *Threatened birds of Asia: the birdlife international red data book*. Cambridge (UK): BirdLife International.
- BirdLife International. 2016. *Otis tarda (great bustard)*. The IUCN Red List of Threatened Species 2016. [cited 2017 Jun 21]. Available from: <http://www.birdlife.org>
- Broderick D, Idaghdour Y, Korrida A, Hellmich J. 2003. Gene flow in great bustard populations across the strait of Gibraltar as elucidated from excremental PCR and mtDNA sequencing. *Conserv Genet*. 4:793–800.
- Collar NJ. 1996. Family Otididae (bustards). In: Del Hoyo J, Elliott A, Sargatal J, editors. *Handbook of birds of the world. Vol. 3: Hoatzin to auks*. Barcelona (Spain): Lynx Edicions. p. 240–273.
- Darriba D, Taboada GL, Doallo R, Posada D. 2012. jModelTest 2: more models, new heuristics and parallel computing. *Nat Methods*. 9:772.
- Drummond AJ, Suchard MA, Xie D, Rambaut A. 2012. Bayesian phylogenetics with BEAUti and the BEAST 1.7. *Mol Biol Evol*. 29:1969–1973.
- Dunning JB Jr. 2008. *CRC handbook of avian body masses*, 2nd ed. Boca Raton (FL): CRC Press.
- Etchécopar RD. 1978. *Birds of China, Mongolia, and Korea. Vol. 2: Non-Passerines*. Papeete (Tahiti): Pacific Editions. In French.
- Excoffier L, Lischer HE. 2010. Arlequin suite ver 3.5: a new series of programs to perform population genetics analyses under Linux and Windows. *Mol Ecol Resour*. 10:564–567.
- Goroshko OA. 2008. Data on the biology of the eastern subspecies of great bustard in Dauria. In: Spitsin VV, editor. *Palaearctic Bustards: breeding and conservation*. Moscow (Russia): Moscow Zoo. p. 130–142. In Russian.
- Hebert PD, Stoeckle MY, Zemlak TS, Francis CM. 2004. Identification of birds through DNA barcodes. *PLoS Biol*. 2:e312.
- Hey J. 2010. Isolation with migration models for more than two populations. *Mol Biol Evol*. 27:905–920.
- Hidalgo de Trucios SJ, Carranza J. 1991. Timing, structure and function of the courtship display in male great bustard. *Ornis Scand*. 22:360–366.
- Idaghdour Y, Broderick D, Korrida A, Chbel F. 2004. Mitochondrial control region diversity of the houbara bustard *Chlamydotis undulata* complex and genetic structure along the Atlantic seaboard of North Africa. *Mol Ecol*. 13:43–54.
- Irisova NL. 2008. Great bustard. In: Irisova N, Malkov N, editors. *Red book of the Altai Republic: animals*. Gorno-Altai (Russia): Gorno-Altai State University. p. 247–250. In Russian.
- Ivanov AI, Kozlova EV, Portenko LA, Tugarinov AY. 1951. *Birds of the USSR, part 1*. Moscow (USSR): Academy of Sciences of the USSR. In Russian.

- Jarvis ED, Mirarab S, Aberer AJ, Li B, Houde P, Li C, Ho SYW, Faircloth BC, Nabholz B, Howard JT, et al. 2014. Whole-genome analyses resolve early branches in the tree of life of modern birds. *Science*. 346:1320–1331.
- Kessler AE. 2015. *Asian great bustards: from conservation biology to sustainable grassland development* [PhD dissertation]. [Tempe (AZ)]: Arizona State University.
- Kessler AE, Batbayar N, Natsagdorj T, Batsuur' D, Smith AT. 2013. Satellite telemetry reveals long-distance migration in the Asian great bustard *Otis tarda dybowskii*. *J Avian Biol*. 44:311–320.
- Kessler AE, Smith AT. 2014. The status of the great bustard (*Otis tarda tarda*) in Central Asia: from the Caspian Sea to the Altai. *Aquila*. 121:115–132.
- Kessler M. 2016. The current status of the great bustard in Central Asia and recommendations for its conservation. *Steppe Bull*. 46:61–69. In Russian.
- Lane SJ, Alonso JC. 2001. Status and extinction probabilities of great bustard (*Otis tarda*) leks in Andalucía, southern Spain. *Biodivers Conserv*. 10:893–910.
- Leigh JW, Bryant D. 2015. popart: full-feature software for haplotype network construction. *Methods Ecol Evol*. 6:1110–1116.
- Librado P, Rozas J. 2009. DnaSP v5: a software for comprehensive analysis of DNA polymorphism data. *Bioinformatics*. 25:1451–1452.
- Lim GS, Balke M, Meier R. 2012. Determining species boundaries in a world full of rarity: singletons, species delimitation methods. *Syst Biol*. 61:165–169.
- Linés Escardó A. 1970. The climate of the Iberian Peninsula. In: Wallén CC, editor. *Climates of northern and western Europe. World series of climatology*. Vol. 5. Amsterdam (Netherlands): Elsevier. p. 195–240.
- Liu G, Hu X, Shafer ABA, Gong M, Han M, Yu C, Zhou J, Bai J, Meng D, Yu G, et al. 2017. Genetic structure and population history of wintering Asian great bustard (*Otis tarda dybowskii*) in China: implications for conservation. *J Ornithol*. 158: 761–772.
- Liu Z, Tian XH, Bai SY. 2007. The genetic diversity and phylogenetic differentiation analysis on two subspecies of *Otis tarda*. *Acta Ecol Sin*. 27:2435–2442. In Chinese.
- Lydolph PE. 1977. *Climates of the Soviet Union. World series of climatology*. Vol. 7. Amsterdam (Netherlands): Elsevier.
- Martín CA, Alonso JC, Alonso JA, Palacín C, Magaña M, Martín B. 2008. Natal dispersal in great bustards: the effect of sex, local population size and spatial isolation. *J Anim Ecol*. 77:326–334.
- Martín CA, Alonso JC, Alonso J, Pitra C, Lieckfeldt D. 2002. Great bustard population structure in central Spain: concordant results from genetic analysis and dispersal study. *Proc Biol Sci*. 269:119–125.
- Mayr G. 2005. A chicken-sized crane precursor from the early oligocene of France. *Naturwissenschaften*. 92:389–393.
- Morales MB, Alonso JC, Martín E, Alonso JA. 2003. Male sexual display and attractiveness in the great bustard *Otis tarda*: the role of body condition. *J Ethol*. 21:51–56.
- Moritz C. 1994. Defining 'evolutionarily significant units' for conservation. *Trends Ecol Evol*. 9:373–375.
- Noriega JI, Tambussi CP. 1995. A late cretaceous presbyornithidae (Aves: Anseriformes) from Vega Island, Antarctic Peninsula: palaeobiogeographic implications. *Ameghiniana*. 32:57–61.
- Olea PP, Casas F, Redpath S, Viñuela J. 2010. Bottoms up: great bustards use the sun to maximise signal efficacy. *Behav Ecol Sociobiol*. 64:927–937.
- Olson SL. 1999. The Anseriform relationships of *Anatalavis Olson* and *Parris* (Anseranatidae), with a new species from the lower eocene London clay. In: Olson SL, editor. *Avian paleontology at the close of the 20th century*. Vol. 89. Proceedings of the 4th International Meeting of the Society of Avian Paleontology and Evolution, 1996 Jun 4–7, Washington, DC. Smithsonian Contributions to Paleobiology. p. 231–243.
- Oparina OS, Litzbarski H, Oparin ML, Vatske Kh, Khrustov AV. 2001. First findings on the migration of great bustards of the Saratov Volga region, obtained through satellite telemetry. In: *Current issues in the research and conservation of birds of Eastern Europe and Northern Asia*. Kazan (Russia): Matbugat Iorty. p. 480–481. In Russian.
- Penteriani V, Delgado MD. 2017. Living in the dark does not mean a blind life: bird and mammal visual communication in dim light. *Philos Trans R Soc London B Biol Sci*. 372:20160064.
- Pereira SL, Baker AJ. 2006. A mitogenomic timescale for birds detects variable phylogenetic rates of molecular evolution and refutes the standard molecular clock. *Mol Biol Evol*. 23:1731–1740.
- Pereira SL, Grau ET, Wajntal A. 2004. Molecular architecture and rates of DNA substitutions of the mitochondrial control region of cracid birds. *Genome*. 47:535–545.
- Pitra C, Watzke H, Lieckfeldt D, Litzbarski H. 2007. Conservation genetics of great bustard in the Ponto-Caspian steppes (Ukraine and the lower Volga basin). *Bustard Stud*. 6:99–110.
- Pons J, Barraclough TG, Gomez-Zurita J, Cardoso A, Duran DP, Hazell S, Kamoun S, Sumlun WD, Vogler AP. 2006. Sequence-based species delimitation for the DNA taxonomy of undescribed insects. *Syst Biol*. 55:595–609.
- Pritchard JK, Stephens M, Donnelly P. 2000. Inference of population structure using multilocus genotype data. *Genetics*. 155:945–959.
- Prum RO, Berv JS, Dornburg A, Field DJ, Townsend JP, Lemmon EM, Lemmon AR. 2015. A comprehensive phylogeny of birds (Aves) using targeted next-generation DNA sequencing. *Nature*. 526:569–573.
- Qiagen, Inc. 2006. Purification of total DNA from nails, hair, or feathers using the DNeasy Blood & Tissue Kit. [cited 2016 Jan 4]. Available from: <https://www.qiagen.com/us/resources/resourcedetail?id=a5a065dc-e287-4a61-b917-9792e25ab42f&lang=en>
- Raab R, Julius E, Greis L, Schütz C, Spakovszky P, Steindl J, Schönemann N. 2014. Endangering factors and their effect on adult great bustards (*Otis tarda*)—conservation efforts in the Austrian LIFE and LIFE+ projects. *Aquila*. 121:49–63.
- Rambaut A. 2009. FigTree, version 1.3. 1. [cited 2016 Jan 4]. Available from: <http://tree.bio.ed.ac.uk/software/figtree>
- Rambaut A, Drummond AJ. 2003. Tracer. [cited 2016 Jan 4]. Available from: <http://tree.bio.ed.ac.uk/software/tracer>
- Rocha P, Marques AT, Moreira F. 2005. Seasonal variation in great bustard *Otis tarda* diet in south Portugal with a focus on the animal component. *Ardeola*. 52:371–376.
- Roselaar CS. 1980. Family Otididae—bustards. In: Cramp S, Simmons KEL, editors. *Handbook of the birds of Europe, the Middle East and North Africa*. Vol. 2: *Hawks to Bustards*. Oxford (UK): Oxford University Press. p. 636–668.
- Sarudny NA. 1905. Eine neue form der Grosstrappe aus Turkestan. *Otis tarda korejewi* subsp. nov. *Ornithol Monatsberichte*. 13:163–164.
- Schüpp M, Schirmer H. 1977. Climates of Central Europe. In: Wallén CC, editor. *Climates of central and southern Europe*. Amsterdam (Netherlands): Elsevier. p. 3–74.
- Spangenberg EP. 1951. Bustard family. In: Dement'ev GP, Meklenburtsev RN, Sudilovskaya AM, Spangenberg EP, editors. *Birds of the Soviet Union*. Vol. 2. Moscow (USSR): Soviet Science. p. 139–168.
- Swofford D. 2002. *PAUP**. Sunderland (MA): Sinauer Associates.
- Taczanowski L. 1874. Second supplement to the report on ornithological investigations of Dr. Dybowski in east Siberia. *J Ornithol*. 22:315–337. In German.
- Tajima F. 1996. The amount of DNA polymorphism maintained in a finite population when the neutral mutation rate varies among sites. *Genetics*. 143:1457–1465.
- Torstrom SM, Pangle KL, Swanson BJ. 2014. Molecular phylogenetics and evolution shedding subspecies: the influence of genetics on reptile subspecies taxonomy. *Mol Phylogenet Evol*. 76:134–143.
- Vaurie C. 1965. *The birds of the Palearctic fauna*. London (UK): Witherby.
- Wang Q, Yan C. 2002. *Chinese cranes, rails and bustard*. Taiwan: National Fenghuang Bird Park.
- Wenink PW, Baker AJ, Tilanus MG. 1993. Hypervariable-control-region sequences reveal global population structuring in a long-distance migrant shorebird, the Dunlin (*Calidris alpina*). *Proc Natl Acad Sci USA*. 90:94–98.
- Wright S. 1931. Evolution in Mendelian populations. *Genet*. 16:97–159.
- Zav'yalov EV, Tabachishin VG, Khrustov AV. 2003. Current understanding of the seasonal migration of great bustards from Saratov Oblast. In: Khrustov AV, editor. *Bustards of Russia and adjacent countries* Vol. 2. Saratov (Russia): Saratov State University. p. 37–47. In Russian.
- Zhao J. 2002. *Studies on breeding ecology of great bustard* [PhD dissertation]. [Shenyang (China)]: Northeast Normal University. In Chinese.